

## Heat and Mass Transfer Analysis due to Mixed Convection in a Rotating Fluid

Farhad Ali

1: Department of Mathematics, Faculty of Science, City University  
of Science & Information Technology, Peshawar, Pakistan.

2: Department of Mathematical Sciences, Faculty of Science, Universiti Teknologi  
Malaysia, 81310 UTM Johor Bahru, Johor, Malaysia

[farhadaliecomaths@yahoo.com](mailto:farhadaliecomaths@yahoo.com)

Samiulhaq

Department of Mathematics, Faculty of Science, City University  
of Science & Information Technology, Peshawar, Pakistan.

[samiulhaqmaths@yahoo.com](mailto:samiulhaqmaths@yahoo.com)

Ilyas Khan

College of Engineering Majmaah University, P. O. Box 66, Majmaah 11952, Saudi  
Arabia.

[ilyaskhanqau@yahoo.com](mailto:ilyaskhanqau@yahoo.com)

Arshad Khan

Department of Mathematics, Faculty of Science, Universiti Teknologi Malaysia,  
81310 UTM Johor Bahru, Johor, Malaysia.

[arsh\\_math@yahoo.com](mailto:arsh_math@yahoo.com)

Asma Khalid

1: Department of Mathematical Sciences, Faculty of Science, Universiti Teknologi  
Malaysia, 81310 UTM Johor Bahru, Johor, Malaysia

2: Department of Mathematics, SBK Women's University, Quetta 87300, Pakistan.

[awaisiasma@gmail.com](mailto:awaisiasma@gmail.com)

### Abstract

This article studies the free convection flow of viscous fluid in a rotating frame. Both heat and mass transfer phenomenon are considered. Magnetohydrodynamic (MHD) fluid over an infinite disk is set into impulsive motion in the presence of thermal radiation and thermal diffusion effects. Exact solutions are obtained using the Laplace transform technique; satisfy all imposed initial and boundary conditions. These solutions are plotted graphically for velocity, temperature and concentration profiles in order to see the effects of the various parameters entering into the problem. The results show that with increasing rotation parameter primary velocity decreases whereas the absolute value of the secondary velocity increases.

### Keywords

MHD, free convection, thermal diffusion, rotating fluid, exact solution.

## 1. Introduction

Study of rotating fluid flows has drawn considerable interest of researchers these days due to its wide range of applications in cosmological and geophysical fluid dynamics, astrophysics, meteorology, petroleum, designing thermo syphon tubes, in cooling turbine blades and in hydrology to study the movement of underground water. Having such motivation, Jana et al. [1] investigated the unsteady flow of viscous fluid through a porous medium bounded by a porous plate in a rotating system. The rotating flows are even more important in the presence of a magnetic field owing to their applications in sunspot development, solar cycle, rotating magnetic stars and in planetary atmosphere research. In view of these applications of the MHD rotating flows, very recently, Farhad et al. [2] extended the work of Jana et al. [1] to the electrically conducting viscous fluid with the consideration of Hall current and slip condition at the boundary. Two other recent attempts considering MHD rotating flows are made by Sahoo et al. [3] and Seth et al. [4].

Despite of the fact that free convection flows are greatly influence by rotation, yet very little attention is given to it in the literature. The Coriolis force, which is a result of a motion of rotating frame, is responsible for the production of rotation in the geofluid. Chandrasekhar [5] pointed out the significant role of the Coriolis force on problems of thermal instability and on stability of viscous flow has made significant contributions to the theory of hydrodynamic flow phenomena in numerous situations. Then, several others studies are carried out by various investigators disclosed that Coriolis force is significant compared to viscous and inertia occurring in the basic equations of the problems involving unsteady free-convection flow past an infinite vertical plate in rotating fluid. Amongst them, the important studies in this direction are made by Singh [6], Bestman and Adjepong [7], Singh et al. [8], Lahurikar [9], Vijayalakshmi[10,11], Nanousis [12], and Mbeledogu and Ogulu [13].

The present article aims to extend the work of Vijayalakshmi [10] to the case of electrically conducting fluid with the inclusion of mass transfer and the thermal diffusion effect as well. Exact solutions of the governing partial differential equations are obtained using the

Laplace transform technique. The influence of the embedded parameters on the flow, thermal and concentration fields are graphically presented and analyzed.

## 2. Mathematical Analysis

We consider unsteady MHD flow of viscous fluid with combined phenomenon of heat and mass transfer are considered together with thermal radiation and thermal diffusion effects. Both the plate and the fluid are in a state of rigid body rotation with uniform angular velocity  $\Omega$  about  $z$ -axis. A uniform magnetic field of strength  $B_0$  is acting perpendicular to the flow i.e along  $z$ -axis in outward direction. Initially ( $t \leq 0$ ), the disk and the fluid are at rest such that the free stream temperature  $T_\infty$  and concentration  $C_\infty$  are the same everywhere. At time  $t > 0$ , the disk starts moving in its own plane with a constant velocity  $U_0$  along the  $x$ -axis. At the same time, the temperature of the plate and concentration are become  $T_w$  and  $C_w$ . Under these assumptions and using Boussinesq approximation, this problem is governed by the following equations (Nanousis[12] and Vijayalakshmi [11])

$$\frac{\partial u'}{\partial t'} - 2\Omega v' = \nu \frac{\partial^2 u'}{\partial z'^2} + g\beta(T' - T_\infty) + g\beta^*(C' - C_\infty) - \frac{\sigma B_0^2}{\rho} u' \quad (1)$$

$$\frac{\partial v'}{\partial t'} + 2\Omega u' = \nu \frac{\partial^2 v'}{\partial z'^2} - \frac{\sigma B_0^2}{\rho} v' \quad (2)$$

$$\rho C_p \frac{\partial T'}{\partial t'} = k \frac{\partial^2 T'}{\partial z'^2} + 16a^* \sigma_1 T_\infty^3 (T_\infty - T') \quad (3)$$

$$\frac{\partial C'}{\partial t'} = D \frac{\partial^2 C'}{\partial z'^2} + \frac{DK_T}{T_m} \frac{\partial^2 T'}{\partial z'^2} \quad (4)$$

where  $\nu$  is the kinematic viscosity,  $t$  is the time,  $g$  is the acceleration due to gravity,  $\beta$  is the volumetric coefficient of thermal expansion,  $\beta^*$  is the volumetric coefficient of mass expansion,  $\sigma$  is the electrical conductivity,  $B_0$  is the applied magnetic field,  $\rho$  is the fluid density,  $C_p$  is the specific heat of the fluid at constant pressure,  $k$  is the thermal conductivity of the fluid,  $D$  is the mass diffusivity,  $K_T$  is the thermal-diffusion ratio,  $T_m$  is the mean fluid temperature,  $a^*$  is the absorption coefficient and  $\sigma_1$  is the Stefan-Boltzmann constant.

Initial and boundary conditions corresponding to this problem are

$$\begin{aligned}
 t' \leq 0 \quad & u' = 0, & T' = T_\infty, & C' = C_\infty & \text{for all } z' \\
 t' > 0 \quad & \begin{cases} u' = U_0, \\ u' = 0, \end{cases} & \begin{cases} T' = T_w, \\ T' \rightarrow T_\infty, \end{cases} & \begin{cases} C' = C_w \\ C' \rightarrow C_\infty \end{cases} & \begin{cases} \text{at } z' = 0 \\ \text{as } z' \rightarrow \infty. \end{cases}
 \end{aligned} \tag{5}$$

Introducing these dimensionless variables

$$\begin{aligned}
 u, v = \frac{u', v'}{U_0}, & \quad z = \frac{z' U_0}{\nu}, & \quad t = \frac{t' U_0^2}{\nu}, \\
 T = \frac{T' - T_\infty}{T_w - T_\infty}, & \quad C = \frac{C' - C_\infty}{C_w - C_\infty},
 \end{aligned} \tag{6}$$

into equations (1)-(5), we get

$$\frac{\partial q}{\partial t} + 2Eqi = \frac{\partial^2 q}{\partial z^2} + G\theta + GrC - mq, \tag{7}$$

$$\frac{\partial T}{\partial t} = \frac{1}{Pr} \frac{\partial^2 T}{\partial z^2} + \frac{R}{Pr} T, \tag{8}$$

$$\frac{\partial C}{\partial t} = \frac{1}{Sc} \frac{\partial^2 C}{\partial z^2} + So \frac{\partial^2 C}{\partial z^2}, \tag{9}$$

$$\begin{aligned}
 t \leq 0 \quad & q = 0, & \theta = 0, & C = 0 & \text{for all } z \\
 t > 0 \quad & \begin{cases} q = 1, \\ q = 0, \end{cases} & \begin{cases} T = 1, \\ T \rightarrow 0, \end{cases} & \begin{cases} C = 1 \\ C \rightarrow 0 \end{cases} & \begin{cases} \text{at } z = 0 \\ \text{as } z \rightarrow \infty, \end{cases}
 \end{aligned} \tag{10}$$

where

$$\begin{aligned}
 q = u + iv, E = \frac{\Omega \nu}{U_0^2}, G = \frac{\nu g \beta (T_w - T_\infty)}{U_0^3}, Gr = \frac{\nu g \beta^* (C_w - C_\infty)}{U_0^3}, \\
 m = \frac{\nu \sigma B_0^2}{\rho U_0^2}, Pr = \frac{\rho \nu C_p}{k}, R = \frac{16a^* \nu^2 \sigma T_\infty^3}{k U_0^2}, Sc = \frac{\nu}{D}, So = \frac{DK_T}{T_m} \frac{(T_w - T_\infty)}{\nu(C_w - C_\infty)},
 \end{aligned}$$

rotation parameter, Grashof number, modified number, magnetic parameter, Prandtl number, radiation parameter, Schmidt number and Soret number respectively.

Solutions of equations (7)-(9) subject to the initial and boundary conditions (13) by the Laplace transform method are

$$\theta(z, t) = \varphi\left(0, \frac{R}{Pr}, z\sqrt{Pr}\right), \tag{11}$$

$$C(z, t) = (1 + A_1)\varphi(0, 0, z\sqrt{Sc}) + A_2\varphi\left(-\frac{R}{Pr - Sc}, 0, z\sqrt{Sc}\right) - A_1\varphi\left(0, \frac{R}{Pr}, z\sqrt{Pr}\right) - A_2\varphi\left(-\frac{R}{Pr - Sc}, \frac{R}{Pr}, z\sqrt{Pr}\right), \quad (12)$$

$$q = (1 + A_3 - A_4)\varphi(0, a, z) - (A_3 + A_5)\varphi\left(-\frac{R - a}{Pr - 1}, a, z\right) + (A_4 + A_5)\varphi\left(\frac{a}{Sc - 1}, a, z\right) - A_3\varphi\left(0, \frac{R}{Pr}, z\sqrt{Pr}\right) + (A_3 + A_5)\varphi\left(-\frac{R - a}{Pr - 1}, \frac{R}{Pr}, z\sqrt{Pr}\right) - A_5\varphi\left(-\frac{R}{Pr - Sc}, \frac{R}{Pr}, z\sqrt{Pr}\right) + A_4\varphi(0, 0, z\sqrt{Sc}) - (A_4 + A_5)\varphi\left(\frac{a}{Sc - 1}, 0, z\sqrt{Sc}\right) + A_5\varphi\left(-\frac{R}{Pr - Sc}, 0, z\sqrt{Sc}\right), \quad (13)$$

where

$$\varphi(x, y, z) = \frac{e^{xz}}{2} [e^{-z\sqrt{x+y}} \operatorname{erfc}\left\{\frac{z}{2\sqrt{t}} - \sqrt{(x+y)t}\right\} + e^{z\sqrt{x+y}} \operatorname{erfc}\left\{\frac{z}{2\sqrt{t}} + \sqrt{(x+y)t}\right\}],$$

$$a = m + 2Ei, \quad A_1 = SoSc, \quad A_2 = \left(\frac{SoScPr}{Pr - Sc} - SoSc\right),$$

$$A_3 = \frac{G - GrSoSc}{R - w}, \quad A_4 = \frac{Gr(1 + SoSc)}{w},$$

$$A_5 = \frac{SoSc^2Gr}{R(Sc - 1) + w(Pr - Sc)}$$

and  $\operatorname{erfc}(x)$  represents the complementary error function.

### 3. Skin Friction, Nusselt Number and Sherwood Number

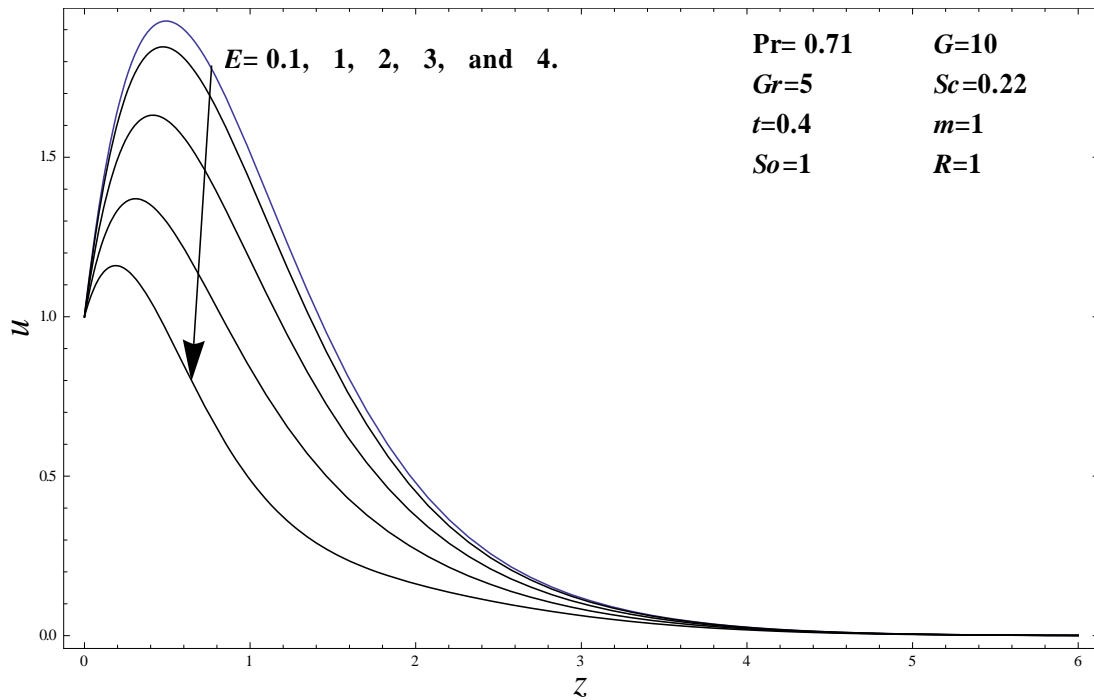
$$\begin{aligned}
\tau = & \left( -\frac{e^{-at}}{\sqrt{\pi t}} - \sqrt{a} \operatorname{erf}\{\sqrt{at}\} \right) + \frac{G - GrScSo}{R - a} \left( \sqrt{R} \operatorname{erf}\left\{ \sqrt{\frac{R}{Pr}} t \right\} \right. \\
& - e^{-\frac{R-a}{Pr-1}t} \sqrt{\frac{aPr-R}{Pr-1}} \operatorname{erf}\left\{ \sqrt{\left( \frac{R}{Pr} - \frac{R-a}{Pr-1} \right) t} \right\} \\
& + e^{-\frac{R-a}{Pr-1}t} \sqrt{\frac{aPr-R}{Pr-1}} \operatorname{erf}\left\{ \sqrt{\frac{aPr-R}{Pr-1}} t \right\} - \sqrt{a} \operatorname{erf}\{\sqrt{at}\} \right) \\
& + \left( \frac{GrSc^2So}{a(Pr-Sc) + R(-1+Sc)} \right) \left( e^{-\frac{R-a}{Pr-1}t} \sqrt{\frac{aPr-R}{Pr-1}} \operatorname{erf}\left\{ \sqrt{\left( \frac{aPr-R}{Pr-1} \right) t} \right\} \right. \\
& - e^{-\frac{R-a}{Pr-1}t} \sqrt{\frac{aPr-R}{Pr-1}} \operatorname{erf}\left\{ \sqrt{\left( \frac{R}{Pr} - \frac{-a+R}{-1+Pr} \right) t} \right\} \\
& - e^{-\frac{at}{Sc-1}} \sqrt{\frac{aSc}{Sc-1}} \operatorname{erf}\left\{ \sqrt{\left( \frac{aSc}{Sc-1} \right) t} \right\} - e^{-\frac{R}{Pr-Sc}t} \sqrt{\frac{RSc}{Pr-Sc}} \operatorname{erf}\left\{ \sqrt{-\frac{Rt}{Pr-Sc}} \right\} \\
& + e^{-\frac{R}{Pr-Sc}t} \sqrt{\frac{ScR}{Pr-Sc}} \operatorname{erf}\left\{ \sqrt{\left( \frac{R}{Pr} - \frac{R}{Pr-Sc} \right) t} \right\} \\
& + e^{\frac{a}{Sc-1}t} \sqrt{\frac{aSc}{Sc-1}} \operatorname{erf}\left\{ \sqrt{\frac{a}{Sc-1}} t \right\} \right) \\
& + \frac{Gr(1+ScSo)}{a} \left( -e^{-\frac{a}{Sc-1}t} \sqrt{\frac{aSc}{Sc-1}} \operatorname{erf}\left\{ \sqrt{\left( \frac{aSc}{Sc-1} \right) t} \right\} \right. \\
& \left. + e^{\frac{a}{Sc-1}t} \sqrt{\frac{aSc}{Sc-1}} \operatorname{erf}\left\{ \sqrt{\frac{a}{Sc-1}} t \right\} + \sqrt{a} \operatorname{erf}\{\sqrt{at}\} \right). \tag{14}
\end{aligned}$$

$$Nu = -\frac{\sqrt{Pr} e^{-\frac{R}{Pr}t}}{\sqrt{\pi t}} - \sqrt{R} \operatorname{erf}\left\{ \sqrt{\frac{R}{Pr}} t \right\}, \tag{15}$$

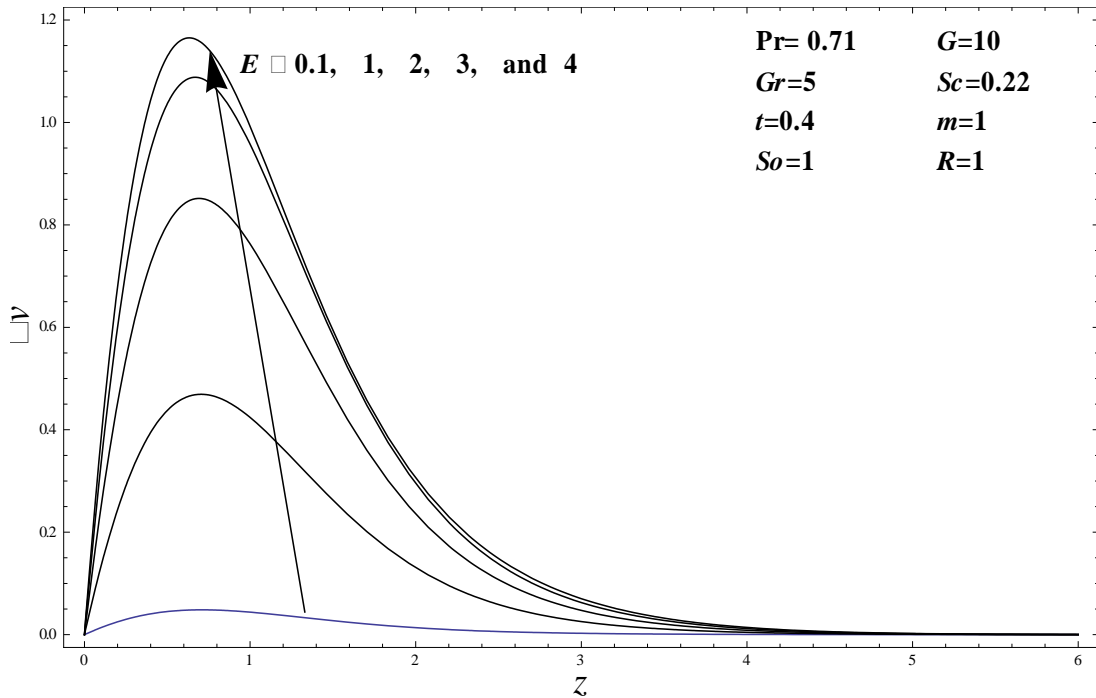
$$\begin{aligned}
Sh = & \frac{\sqrt{Sc}}{\sqrt{\pi t}} - ScSo \left( \sqrt{R} \operatorname{erf}\left\{ \sqrt{\frac{R}{Pr}} t \right\} - e^{-\frac{R}{Pr-Sc}t} \sqrt{\frac{ScR}{Sc-Pr}} \operatorname{erf}\left\{ \sqrt{\left( \frac{R}{Pr} - \frac{R}{Pr-Sc} \right) t} \right\} \right. \\
& + e^{-\frac{R}{Pr-Sc}t} \sqrt{\frac{RSc}{Sc-Pr}} \operatorname{erf}\left\{ \sqrt{\left( \frac{R}{Sc-Pr} \right) t} \right\} \\
& - \left( \frac{PrScSo}{Pr-Sc} \right) \left( e^{-\frac{R}{Pr}t} \sqrt{\frac{Pr}{\pi t}} + e^{-\frac{R}{Pr-Sc}t} \sqrt{\frac{ScR}{Sc-Pr}} \operatorname{erf}\left\{ \sqrt{\left( \frac{R}{Pr} - \frac{R}{Pr-Sc} \right) t} \right\} \right. \\
& \left. - \sqrt{\frac{Sc}{\pi t}} - e^{-\frac{R}{Pr-Sc}t} \sqrt{\frac{RSc}{Sc-Pr}} \operatorname{erf}\left\{ \sqrt{\left( \frac{R}{Sc-Pr} \right) t} \right\} \right). \tag{16}
\end{aligned}$$

#### 4. Graphical Results and Discussion

Graphical results are plotted to see the behavior of various embedded parameters on non-dimensional velocity components  $u$  and  $v$ , temperature  $T$  and concentration  $C$ . The Prandtl number  $Pr=0.71$ , corresponds to air, is used throughout numerical computation. Moreover, the Grashof number  $G$  and the modified Grashof number  $Gr$  are chosen equal to 10 and 5 respectively. On the other hand, the value of the Schmidt number  $Sc$  is taken as 0.22, which corresponds to  $H_2$ , with air as the solvent and the magnetic parameter  $m=1$  is selected. The values of the Radiation parameter  $R$ , Soret parameter  $So$  and Rotation parameter  $E$  are chosen arbitrarily.



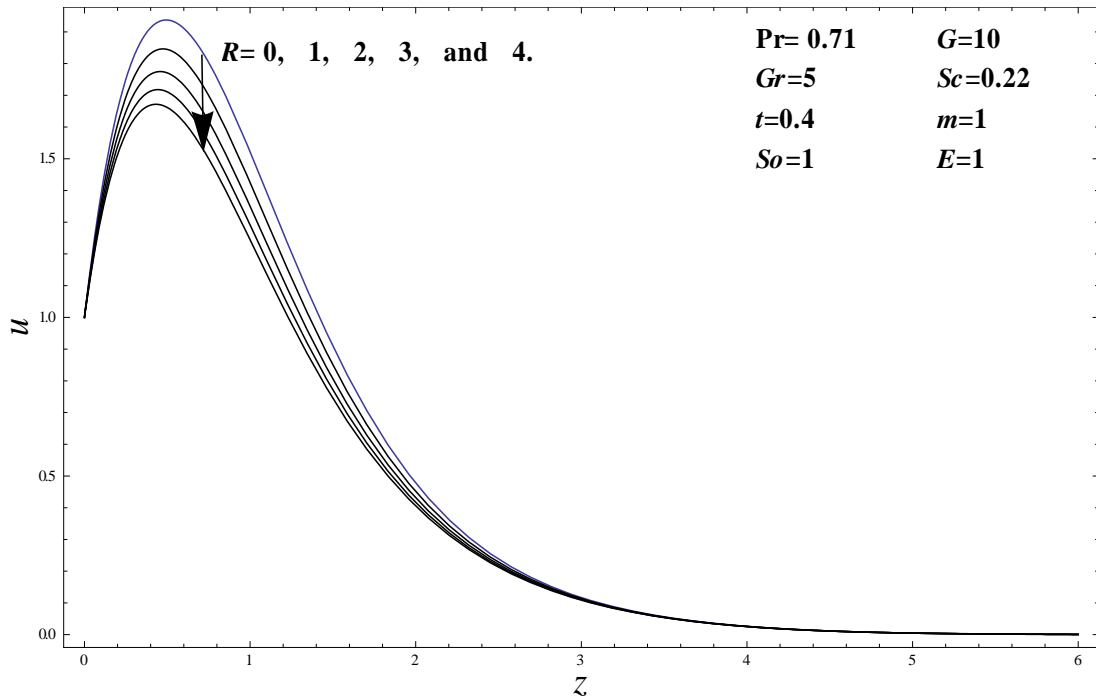
**Figure 4.1(a)** Primary velocity profile  $u$  against  $z$  for different rotation parameter,  $E$ .



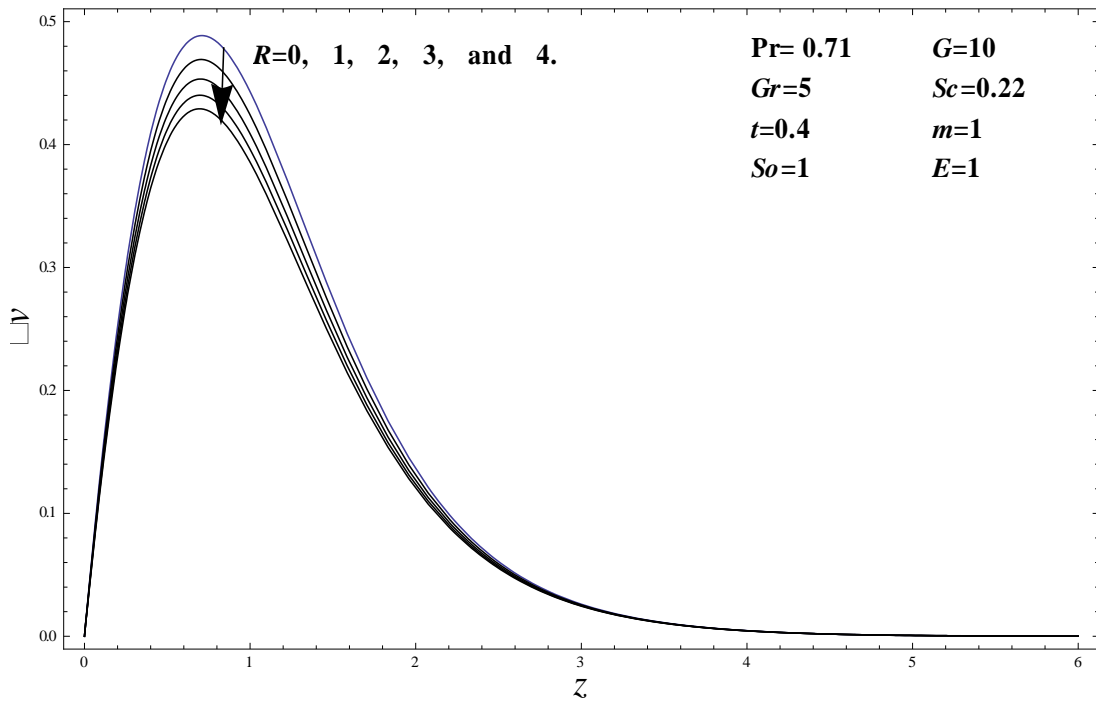
**Figure 4.1(b)** Secondary velocity profile  $v$  against  $z$  for different rotation parameter,  $E$ .

Figure 4.1(a) and Figure 4.1(b) illustrate that the primary velocity  $v$  decreases whereas the absolute value of the secondary velocity increases near the plate and tend to zero away from the plate with an increase in rotation parameter. This implies that rotation retards the primary velocity whereas it accelerates the secondary velocity. This may be attributed to the fact that when the frictional layer near the plate is suddenly set into motion then the Coriolis force acts as a constraint in the main fluid flow to induce cross flow in the flow field. Figure 4.1(b) shows that the influence of the rotation parameter  $E$  on the secondary velocity is significant near the plate. A small increase in the value of  $E$  will cause the secondary velocity to decrease rapidly.





**Figure 4.2(a)** Primary velocity profile  $u$  against  $z$  for different radiation parameter,  $R$ .



**Figure 4.2(b)** Secondary velocity profile  $v$  against  $z$  for different radiation parameter,  $R$ .

Figure 4.2(a) shows that with an increase in the radiation parameter  $R$ , the primary velocity  $u$  decreases in the presence of radiation as well as in the case of pure convection.

Numerically for pure convection we take  $R \rightarrow 0$ , i.e. the radiation effect is negligible. Moreover, the absolute value of the secondary velocity in the presence of radiation as well as in the case of pure convection, decreases near the plate for increasing values of the radiation parameter  $R$  as can be seen from Figure 4.2(b). Moreover, it is observed that in case of pure convection  $R \rightarrow 0$ , the momentum boundary layer is greater results in a greater velocity and approaches to zero asymptotically. This fact is in accordance with the physical situation that increasing the radiation parameter contributes in the thickening of boundary layer.

The temperature profiles for air,  $Pr=0.71$  are calculated for different values of radiation parameter  $R$  from equation (14) with time,  $t=0.4$  and are presented in Figure 4.4. It is observed from this figure that temperature and thermal boundary layer thickness decrease with increasing radiation parameter  $R$ . Physically, it is true due to the fact that increasing radiation parameter  $R$  makes the fluid thicken, ultimately causing the temperature and the thermal boundary layer thickness to decrease.

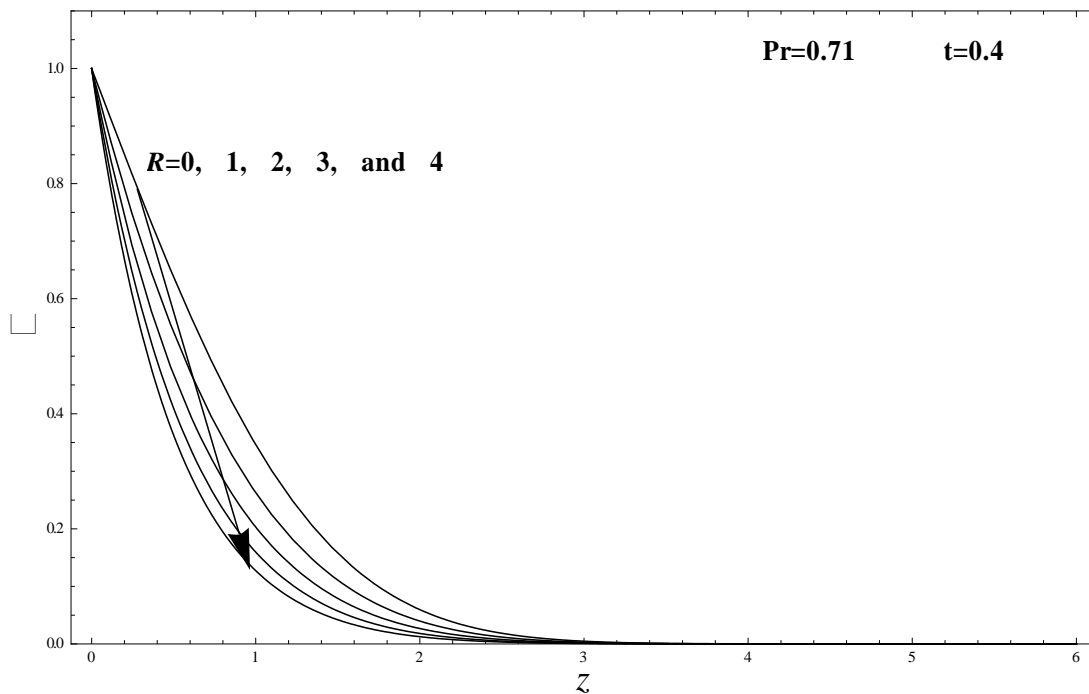


**Figure 4.3** Profile of non-dimensional temperature  $\theta$  for different values of radiation parameter  $R$ .

Effect of different Soret number on the concentration profiles is shown in Figure 4.5. We observed that the influence of the Soret number on the concentration profiles is significant. Concentration profiles increase with increasing values of the Soret number.

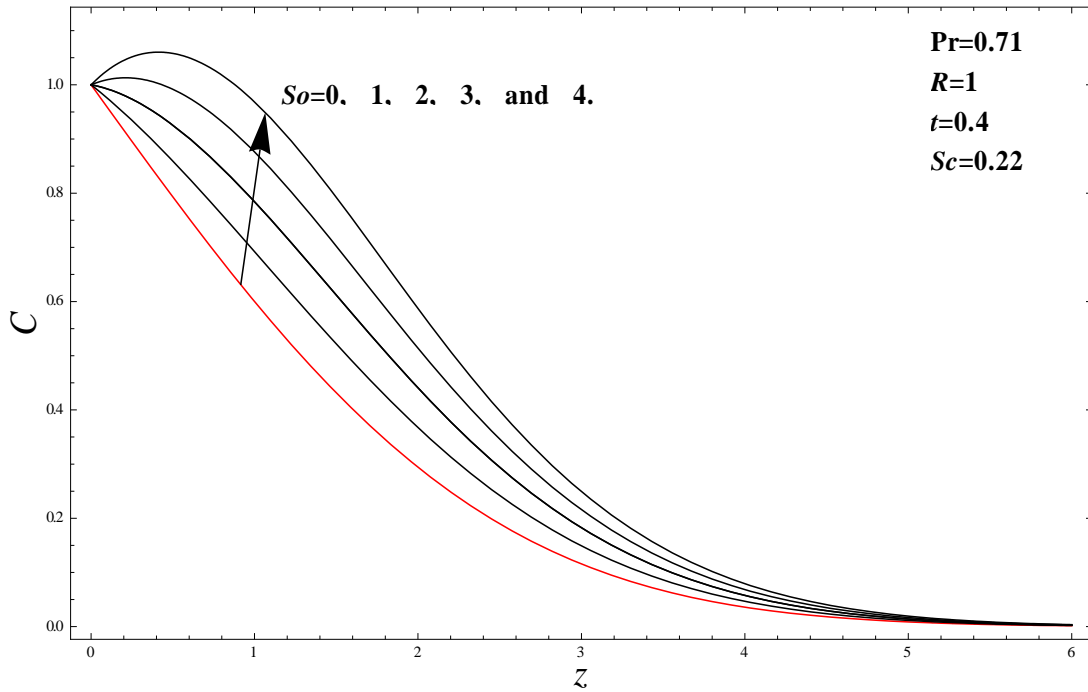


**Figure 4.4** Profile of non-dimensional concentration  $C$  for different values of Soret number  $So$ .

## 5. Conclusion

Exact solutions for the rotating MHD free convection flow of viscous fluid with heat and mass transfer over an impulsively started infinite vertical plate in the presence of thermal radiation and thermal diffusion are obtained. It is found that they satisfy all imposed initial and boundary conditions and can be reduced as a special case to other well-established results in the literature. From the graphical results of the fluid velocity, temperature and concentration, we found that the embedded parameters have strong influence on the present problem.

References:

- [1] M. Jana, S.L. Maji, S. Das and R.N. Jana, Unsteady flow of viscous fluid through a porous medium bounded by a porous plate in a rotating system, *J. Porous Media*, 13, (2010) 645-70.
- [2] A. Farhad, M. Norzieha, S. Sharidan, I. Khan and Samiulhaq, Hydromagnetic rotating flow in a porous medium with slip condition and Hall current, *Int. J. Phys. Sci.* 7 (2012) 1540-1548.
- [3] S.N. Sahoo, J.P. Panda and G.C. Dash, Hydromagnetic oscillatory flow and heat transfer of a viscous liquid past a vertical porous plate in a rotating medium, *Indian J. Sci. Technol.* 3, (2010) 817.
- [4] G.S. Seth, M.S. Ansari and R. Nandkeolyar, Unsteady Hydromagnetic Couette flow within porous plates in a rotating system, *Adv. Appl. Math. Mech.* 2, (2010), 286.
- [5] S. Chandrasekhar. *Hydrodynamic and Hydromagnetic Stability*, Oxford University Press, London (1961).
- [6] K. Singh, Hydromagnetic Free Convection Flow Past an Impulsively Started Vertical Plate in a Rotating Fluid, *Int. Com. Heat Mass Transf.* 11 (1983) 399-406.
- [7] R. Bestman and S. K. Adjepong, Unsteady Hydromagnetic Free Convection Flow with Radiative Heat Transfer in a Rotating Fluid, *Astrophysics and Space Science*, 143 (1988) 73-80.
- [8] J. N. Singh Sing and A. K. Sing, Transient Hydromagnetic Free Convection Flow Past an Impulsively Started Vertical Plate, *Astrophysics and Space Science*, 176 (1991) 97-104.
- [9] R. M. Lahurikar, On Flow Past an Impulsively Started Infinite Vertical Isothermal Plate in a Rotating Fluid Solution, *Bulletin of Malaysia Mathematical Society*, 11,1 (2010) 41-49.
- [10] R. Vijayalakshmi, Radiation Effects on Free Convection Flow Past an Impulsively Started Vertical Plate in a Rotating Fluid, *Theoret. Appl. Mech.*, 37, 2 (2010) 79-95.
- [11] R. Vijayalakshmi and A.P.F. Kamalam, Free Convection Flow Past an Accelerated Vertical Plate with Thermal Radiation in a Rotating Fluid, *Int. T. Pur Appl. Math Sci*, 5 (2012) 43-51.
- [12] N. Nanousis, Thermal Diffusion Effects on MHD Free Convective and Mass Transfer Flow Past a Moving Infinite Vertical Plate in a Rotating Fluid. *Astrophysics and Space Science*, 191(1992)313-322.
- [13] U. Mbeledoguan and A. Ogulu, Heat and Mass Transfer of an Unsteady MHD Natural Convection Flow of a Rotating Fluid Past a Vertical Porous Flat Plate in the Presence of Radiative Heat Transfer, *Int. J Heat Mass Transf.* 50(2007)1902-1908.